



Patterns and controls of carbon dioxide concentration and fluxes at the air–water interface in South American lowland streams

Claudia Feijó^{1,2} · Maite Arroita³ · María Laura Messetta^{1,2} · Julieta Anselmo¹ · Laura Rigacci¹ · Daniel von Schiller⁴

Received: 23 September 2021 / Accepted: 10 February 2022 / Published online: 25 March 2022
© The Author(s), under exclusive licence to Springer Nature Switzerland AG 2022

Abstract

Carbon dioxide (CO₂) emission from fluvial systems represents a substantial flux in the global carbon cycle. However, variation in fluvial CO₂ fluxes at the air–water interface as well as its drivers are poorly understood, especially in non-forested headwaters. Here, we measured CO₂ concentration and fluxes in 14 lowland open-canopy streams (Pampean region, Argentina) that cover a wide range of land use and water quality. We also analyzed drivers of CO₂ concentration and fluxes, including factors related to metabolism, gas solubility, alkalinity, and gas transfer. Metabolic rates varied considerably among the study sites, but most streams (i.e., 8 out of the 11 where we were able to estimate ecosystem metabolism) were net heterotrophic. Metabolic differences among sites were mostly driven by the aromatic carbon content and the percent of the stream reach covered by primary producers. All streams, even those that were not net heterotrophic were CO₂ supersaturated. Alkalinity combined with in-stream primary production explained 52.3% of the variance in the partial pressure of CO₂ (*p*CO₂), but our observations suggest that *p*CO₂ might be controlled by external groundwater inputs of dissolved inorganic carbon rather than by internal metabolism. All streams were net emitters of CO₂ to the atmosphere. Significantly more variance in CO₂ flux was explained by gas transfer velocity (63.7%) than by *p*CO₂ (21.9%). We also observed high spatial heterogeneity in CO₂ fluxes within each stream, which was associated with flow variation and the presence of different macrophyte and algae patches. Overall, our results indicate that CO₂ emission in these extremely low turbulence streams is controlled by a combination of external and internal biogeochemical processes and limited atmospheric exchange.

Keywords CO₂ · *p*CO₂ · Emission · Evasion · Metabolism · Macrophytes

Introduction

Fluvial ecosystems play a central role in the global carbon cycle (Cole et al. 2007; Aufdenkampe et al. 2011; Raymond et al. 2013; Regnier et al. 2013). Despite occupying < 1% of

the terrestrial surface (Allen and Pavelsky 2018), streams and rivers can release ~ 1.8 Pg C y⁻¹ in the form of carbon dioxide (CO₂) to the atmosphere, exceeding the CO₂ emissions from lakes and reservoirs (Raymond et al. 2013). In particular, the contribution of small streams to CO₂ emission is not completely understood, but conservative estimates suggest that 36% of total fluvial CO₂ outgassing may be accounted for by these systems (Marx et al. 2017).

The exchange of CO₂ across the air–water interface depends on the gas transfer velocity and the partial pressure of CO₂ (*p*CO₂) at the water surface (Alin et al. 2011; Raymond et al. 2013). The gas transfer velocity is controlled by surface water turbulence that, in turn, is strongly related to geomorphic and hydraulic variables, such as stream channel slope and stream flow velocity (Raymond et al. 2012; Hall and Ulseth 2020). The magnitude of *p*CO₂ relies on both external and internal dissolved inorganic carbon (DIC) sources (Hotchkiss et al. 2015). External DIC

✉ Claudia Feijó
clasife@yahoo.com.ar

¹ Departamento de Ciencias Básicas, Instituto de Ecología y Desarrollo Sustentable (CONICET-UNLU-CIC), Universidad Nacional de Luján, Luján, Argentina
² CONICET, Buenos Aires, Argentina
³ Department of Plant Biology and Ecology, Faculty of Science and Technology, University of the Basque Country, Bilbao, Spain
⁴ Department of Evolutionary Biology, Ecology and Environmental Sciences, University of Barcelona, Barcelona, Spain

sources include soil respiration and weathering of minerals in the catchment that enter streams via groundwater inputs, whereas internal DIC sources include in-stream photochemical mineralization and ecosystem respiration. In general, external sources contribute more than internal sources to CO₂ emissions from low-order streams, which tend to be supersaturated with CO₂ compared to the overlying atmosphere (Hotchkiss et al. 2015; Marx et al. 2017; Demars 2019). Net ecosystem production (NEP) may increase *p*CO₂ in the stream water when ecosystem respiration exceeds gross primary production, and thus, NEP is negative (Jones and Mulholland 1998; Duarte and Prairie 2005; Hotchkiss et al. 2015). However, internal metabolism typically accounts for <20% of total CO₂ evasion from streams to the atmosphere, and this contribution may increase with stream order (Butman and Raymond 2011; Hotchkiss et al. 2015; Gómez-Gener et al. 2016; Hill et al. 2017; Demars 2019).

Knowledge on CO₂ dynamics in streams is based mostly on data from forested headwaters of the northern hemisphere, whereas other stream types and regions remain understudied (Lauerwald et al. 2015). In South America, for instance, there are few studies on CO₂ dynamics from lowland streams (except for Amazonian fluvial systems). These prevalent freshwater ecosystems are characterized by slow-flowing waters, lack of riparian forest, high irradiance, dense assemblages of macrophytes, and high primary production, especially in summer (Feijó and Lombardo 2007; García et al. 2017). These features, which resemble those of nutrient-rich, lowland streams elsewhere in the world, may strongly affect the dynamics of CO₂. Low water turbulence strongly reduces CO₂ exchange by decreasing the gas transfer velocity between water and atmosphere (Hall and Ulseth 2020). This effect is enhanced in the presence of floating macrophytes, which further diminish physical gas exchange (Attermeyer et al. 2016; Peixoto et al. 2016). In addition, primary production and respiration of macrophytes strongly influence stream metabolism in lowland streams, leading to high ecosystem metabolic rates (García et al. 2017; Alnoe et al. 2021). Thus, the physical and metabolic consequences of macrophyte presence are expected to significantly influence *p*CO₂ and CO₂ exchange (Attermeyer et al. 2016; Peixoto et al. 2016; Pu et al. 2017). Finally, high irradiance can also influence CO₂ dynamics by enhancing the photochemical mineralization of organic matter and primary production (Lu et al. 2013).

In this study, we examined the magnitude and drivers of *p*CO₂ and CO₂ exchange at the air–water interface in lowland Pampean streams covering a wide range of catchment land uses, water physicochemical characteristics, and rates of ecosystem metabolism. We predicted that the study streams would be saturated with CO₂ compared to the overlying atmosphere, and that metabolism would contribute significantly to *p*CO₂. We further predicted that, despite

high *p*CO₂, slow current velocities and low water turbulence would strongly restrict CO₂ exchange between water and atmosphere. Finally, we predicted that low current velocities and high abundance and diversity of emergent, submerged, and floating macrophytes would enhance the spatial heterogeneity of CO₂ exchange within stream reaches.

Materials and methods

Study sites

We sampled 14 streams of the Pampean region (Buenos Aires province, Argentina) (Fig. 1). The region is covered by a sequence of sands and loess deposited during the Tertiary and the Quaternary (Sala et al. 1983). Relief is flat (0–200 m above sea level) in most parts of the province. Climate is temperate humid, with a mean annual temperature between 13 and 17 °C and a mean annual rainfall between 700 and 1200 mm evenly distributed throughout the year (Matteucci 2012). Due to the expansion of agriculture and cattle breeding, natural vegetation (mostly grasslands) is confined to small patches in less-productive lands and in riparian zones. Stream sediments consist mainly of fine materials (silt and clay).

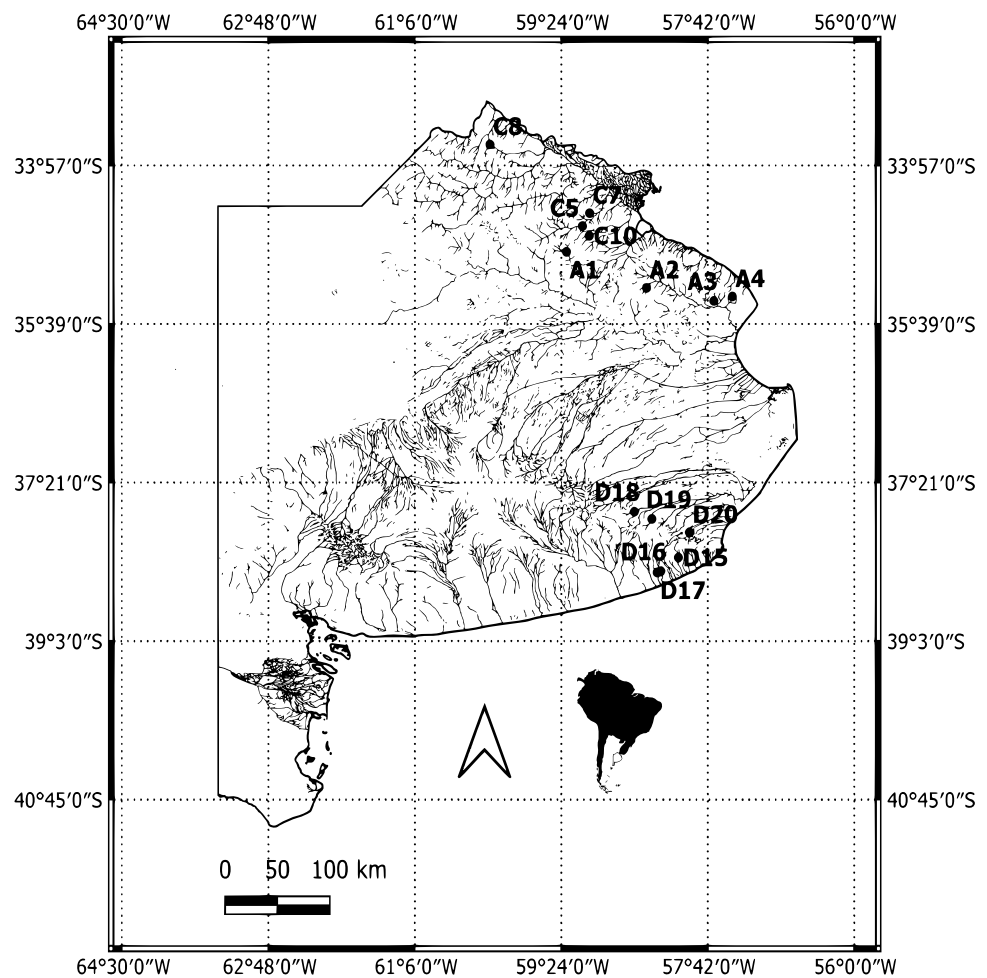
To cover a wide range in physicochemical conditions, we selected streams from three ecoregions of the Buenos Aires province: Salado River and tributaries, tributaries of the Paraná and Río de la Plata Rivers, and tributaries of the Atlantic Ocean [regions A, C, and D, respectively, according to Feijó and Lombardo (2007)]. Ecoregions differ in geomorphologic and hydrological features (Frenguelli 1956). The Salado River system runs along a tectonic depression forming wandering meanders. Tributaries of the Paraná and Río de la Plata Rivers have well defined drainage networks and steeper banks compared to the other systems. Tributaries of the Atlantic Ocean are characterized by scarcely marked channels in the upper and middle reaches that become deeper downstream, forming steep banks close to the mouth. Rivers of this region tend to run separately, without forming common branches.

The catchments of the selected streams differed significantly in cropland (cropland = 5.8–92.6%) and cattle (0.4–72.6%) land use (Supplementary Table 1). Land-use data were derived from Landsat V Thematic Mapper (TM) satellite images (provided by the Instituto Nacional de Pesquisas Espaciais, INPE, Brazil).

Stream reach characterization

We sampled between February and March 2019 (austral summer). Each stream was visited on one occasion and sampled between 12 and 16 h, when metabolic activity is highest (Martí et al. 2020).

Fig. 1 Location of the 14 sampled streams in three ecoregions of Buenos Aires province, Argentina. **a** Salado River and tributaries, **c** Tributaries of the Paraná a Río de la Plata Rivers, and **d** Tributaries of the Atlantic Ocean



We selected a 100-m reach at each stream. At the end of the reach, we measured stream cross-sectional area with a ruler and tape measure as well as current velocity with a Schiltknecht MiniAir20 anemometer (Schiltknecht Messtechnik, Gossau, Switzerland) to estimate stream discharge by the velocity–area method (Gordon et al. 1992). We measured wetted width in ten transects separated 10 m away to determine reach surface area. In each transect, we also measured depth in triplicate (at the center and close to the margins) to calculate mean reach depth.

We mapped macrophyte abundance by visually estimating the percent of the stream reach covered by each plant species in 5-m sub-reaches. These data were then used to calculate the percent of reach surface covered by different life forms (macroalgae and emergent, submerged, and floating macrophytes) (Feijóo et al. 2011).

Water physicochemistry

We measured water temperature, conductivity, and pH in situ at the middle of the reach of each stream with a

Hach HQ40D multiprobe (Hach Company, Loveland, CO, USA). We calibrated the probes following the manufacturer's instructions at the start of the sampling campaign and checked them before every visit to the field. In the same spot, we also collected three water samples (250-mL acid-washed polyethylene bottles), which were stored in an ice chest and transported to the laboratory for later analyses.

We used one unfiltered sample to determine alkalinity (carbonates and bicarbonates) by titration (APHA 2005, method code 2320 B) within the same day of collection.

We filtered the second sample through pre-ashed glass fiber filters (Whatman GF/F, nominal pore size = 0.7 μm) preserved it with 0.1% chloroform, and stored it at 4 $^{\circ}\text{C}$ until nutrient analysis (Gardolinski et al. 2001). We estimated soluble reactive phosphorus (SRP) and ammonium concentrations by the molybdate–ascorbic method and the indophenol blue method, respectively (APHA 2005). We determined nitrate and nitrite concentrations with a FUTURA Autoanalyzer (Alliance Instruments, Frepillon, France) through a reaction with sulfanilamide with a previous Cu–Cd reduction for nitrate (APHA 2005).

We filtered the third sample through pre-ashed glass fiber filters (Whatman GF/F, nominal pore size = 0.7 μm), and divided it into two subsamples. We stored the first subsample in amber-colored glass bottles to minimize light exposure, acidified it with HCl 10% to reach pH 2, and analyzed it for dissolved organic carbon (DOC) by high-temperature catalytic oxidation on a Shimadzu TOC-V CSH Analyzer (Shimadzu Corporation, Kyoto, Japan). We filtered the second subsample through 0.2- μm nylon membrane filters (GVS Magna, Bologna, Italy) and kept it in cool and dark conditions for the spectroscopic analysis of dissolved organic matter (DOM) composition (Spencer et al. 2014).

We measured the absorbance spectra (200–800 nm) on a Shimadzu UV-1800 spectrophotometer (Shimadzu Corporation, Kyoto, Japan) using a 1-cm quartz cuvette. We used Milli-Q water as blank and subtracted the average sample absorbance between 700 and 800 nm from the spectrum to correct for offsets due to instrument baseline drift (Green and Blough 1994). We determined the specific UV absorbance at 254 nm (SUVA, $\text{L mg}^{-1} \text{m}^{-1}$) by dividing the UV absorbance measured at 254 nm by the DOC concentration (Weishaar et al. 2003). The SUVA index is associated with bulk aromaticity in the sample, with higher values being indicative of a high content of aromatic carbon. We determined the spectral slopes for the interval 275–295 and 350–400 nm (S_{275–295} and S_{350–400}, respectively) by fitting the single absorbance spectra to an exponential decay function. We calculated the slope ratio (SR) as the ratio of S_{275–295} to S_{350–400}, with high values of the index indicative of low molecular weight compounds (Helms et al. 2008).

We further analyzed DOM composition via Excitation–Emission Matrices (EEMs) using a Perkin Elmer LS 55 fluorescence spectrophotometer (Perkin Elmer, Waltham, MA, USA) with a 1-cm quartz cuvette. We measured fluorescence intensity across the excitation range set from 240 to 449 nm (3 nm increments) and the emission range set from 250 to 598 nm (3 nm increments). Before measuring the samples, we calibrated the fluorometer with a Rhodamine B solution to correct instrument-specific biases. We allowed water samples to warm to room temperature prior to measurements. EEMs were blank subtracted using the EEM of Milli-Q water, determined every ten samples. We corrected spectra for inner filter effects using UV–Vis absorbance spectra (Kothawala et al. 2013). We calculated three DOM descriptors: (i) humification index (HIX), with higher values indicating higher humification degree (Fellman et al. 2010); (ii) biological index (BIX), related to the proportion of recently produced DOM, for which higher values are indicative of a higher contribution of recently produced DOM (Hughes et al. 2009); and (iii) fluorescence index (FI), related to DOM sources, with values ranging between ~1.2 for higher plant DOM sources to ~1.8 for microbial DOM sources (Cory and McKnight 2005).

Whole-stream metabolism

We estimated whole-stream rates of gross primary production (GPP) and ecosystem respiration (ER) with the open-channel one-station technique (Odum 1956; Uehlinger and Naegeli 1998). The day before the sampling, we installed a field-calibrated oximeter (HQ40D, Hach, Loveland, Colorado; miniDOT, PME, Vista, California) at the end of the stream reach. We measured changes in dissolved oxygen (DO) concentration (mg L^{-1}) and water temperature ($^{\circ}\text{C}$) in 5-min intervals for 24 h. For all sites situated in the north of the province (all A and C sites, except C8; Fig. 1), we obtained photosynthetically active radiation (PAR, 400–700 nm, $\mu\text{mol m}^{-2} \text{s}^{-1}$) from the meteorological station in Lujan. For the rest of the sites (C8 and all D sites; Fig. 1), we modeled light based on latitude and longitude (Appling et al. 2017). We also obtained barometric pressure (mb) from nearby meteorological stations (Lujan for the A and C sites in the north, Balcarce and Miramar for the D sites in the south of the province). The distance from the meteorological station to the furthest stream was 194 km. We used barometric pressure together with water temperature to estimate the DO saturation concentration (i.e., the theoretical concentration of DO if the air and water were at equilibrium; mg L^{-1}) (García and Gordon 1992; Colt 2012). Mean stream depth (m) was obtained from transects (see above).

We estimated GPP ($\text{g O}_2 \text{m}^{-2} \text{d}^{-1}$), ER ($\text{g O}_2 \text{m}^{-2} \text{d}^{-1}$) and K_{600} (i.e., the gas exchange rate coefficient after normalization for molecular properties and temperature to a Schmidt number of 600, corresponding to DO at 17.5 $^{\circ}\text{C}$; d^{-1}) fitting models of DO dynamics to DO data, using inverse fitting and Bayesian inference (Holtgrieve et al. 2010). The gas transfer velocity (k_{600} , m d^{-1}) was calculated multiplying K_{600} (d^{-1}) by mean stream depth (m). The model we used corresponded to the model variant `b_np_oipi_tr_plrckm.stan` in the stream-Metabolizer R package (Appling et al. 2017), which accounts for both observation and process errors in diel DO dynamics using a state space formulation. The most likely sources of process error in our streams are inputs of low- O_2 groundwater, the high patchiness of primary producers and light-associated misspecifications (in particular, cloudiness at sites C8 and D15-D20, where we modeled light based on latitude and longitude). The process error accounts for these misspecifications and besides, including both observation and process errors, which provides lower bias and more accurate estimates of parameter error than assuming either process error or observation error alone (Appling et al. 2018).

Prior probability values for parameters were based on literature range from Hall et al. (2016), following Appling et al. (2018). Priors were $\text{GPP} \sim \text{N}(3.1, 6.0)$, $\text{ER} \sim \text{N}(7.1, 7.1)$, and $K_{600} \sim \text{Lognormal}(2.48, 1.0)$. Tests on subsets of the data showed that the posterior parameter distribution was robust to varying these priors.

We solved for model parameters using program Stan, a Markov chain Monte Carlo (MCMC) simulation program (Stan Development Team 2016). This method was embedded in streamMetabolizer version 0.11.4 and R version 3.6.3. We ran four MCMC chains in parallel on four cores, with 1000 warmup steps and 500 saved steps on each chain.

To assess model fit, we ensured parameter convergence as the Gelman-Rubin Rhat < 1.1. We also checked how well modeled DO fitted observed DO. Although all models converged, we excluded estimates at A3, A4, and D16 because of poor model fit.

pCO₂ and CO₂ exchange

We measured the partial pressures of CO₂ in water and air (*p*CO_{2,w} and *p*CO_{2,a}, respectively) in three points along the stream reach. To capture stream reach heterogeneity, each selected point presented different biological community composition (algae, macrophytes, or open water) and hydraulic conditions (current velocity, measured with a Schiltknecht MiniAir20 anemometer).

We made measurements by triplicate at each location using an infrared gas analyzer (EGM-4, PP-Systems, USA). For *p*CO_{2,w} measurements, we circulated water samples at a rate of ~300 mL min⁻¹ through a membrane contactor (MiniModule, Liquid-Cel, USA) coupled to the gas analyzer (Gómez-Gener et al. 2016). For *p*CO_{2,a}, we circulated atmospheric air approximately 1 m above the water surface through the gas analyzer.

We determined CO₂ exchange across the water–air interface (mmol m⁻² d⁻¹) using an indirect and a direct approach. The CO₂ exchange estimated with the indirect approach (CO₂ exchange_(indirect)) provided an average estimation of the CO₂ exchange at reach scale, whereas the CO₂ exchange estimated with the direct approach (CO₂ exchange_(direct)) allowed exploring the spatial heterogeneity in CO₂ exchange along the reach. Positive values of CO₂ exchange indicate that the stream behaved as a net CO₂ emitter (i.e., there is an efflux of the gas to the atmosphere), whereas negative values indicate that the stream was a CO₂ sink.

We determined CO₂ exchange_(indirect) using Fick's law of gas diffusion

$$\text{CO}_2\text{exchange}_{(\text{indirect})} = k_{\text{CO}_2} K_h (p\text{CO}_{2,w} - p\text{CO}_{2,a}), \quad (1)$$

where k_{CO_2} (m d⁻¹) is the specific gas transfer velocity for CO₂, K_h (mmol µatm⁻¹ m⁻³) is Henry's constant for CO₂ adjusted for salinity and temperature, and *p*CO_{2,w} (µatm) and *p*CO_{2,a} (µatm) are the partial pressures of CO₂ in water and air, respectively. We made measurements of *p*CO₂ by triplicate at each location. We estimated k_{CO_2} using the k_{600}

estimated with the metabolism model and the Schmidt number of CO₂ at the stream water temperature during *p*CO_{2,w} measurements (Raymond et al. 2012).

We determined CO₂ exchange_(direct) using the enclosed chamber method (Goldenfum 2010) at the same locations where we measured *p*CO_{2,w} and *p*CO_{2,a}. We made measurements by triplicate at each location. We monitored the CO₂ gas concentration inside an opaque floating chamber every 4.8 s with the infrared gas analyzer. Exchange measurements lasted until we observed a change in CO₂ of at least 10 µatm, with a minimum duration of 120 s and a maximum of 240 s. We estimated CO₂ exchange_(direct) (mmol m⁻² d⁻¹) from the rate of change of CO₂ inside the chamber as

$$\text{CO}_2\text{exchange}_{(\text{direct})} = \left(\frac{d\text{CO}_2}{dt} \right) \left(\frac{V}{RTS} \right), \quad (2)$$

where $\left(\frac{d\text{CO}_2}{dt} \right)$ is the slope of the relationship between CO₂ concentration and time (µatm s⁻¹), V and S are the volume and the surface area of the chamber (3.37 dm³ and 4.14 dm², respectively), T is the air temperature (K), and R is the ideal gas constant (0.08206 L atm K⁻¹ mol⁻¹) (Bodmer et al. 2016; Gómez-Gener et al. 2016).

Statistical analyses

We performed all statistical analyses using the R software version 3.6.3 (R Core Team 2021).

We used a principal component analysis (PCA) to identify stressor gradients in the data, detect the main environmental differences among the study streams, and analyze correlations between variables (Johnson and Hering 2009). Before conducting the PCA, we reduced the number of variables. For land use, we used percent agriculture, because together with cattle, it is the main land use in all the catchments and both were inversely related (i.e., the higher the cover of agriculture, the lower the cover of cattle, and vice versa). For nutrient status, we used dissolved inorganic nitrogen (DIN; the sum of NH₄, NO₃, and NO₂), SRP, and DOC. For hydro-morphology, we used discharge, which strongly correlated with both water depth and current velocity. For primary producers, we used the percent of the stream reach covered by primary producers (i.e., the sum of the percent of algae and emergent, submerged and floating macrophytes). For physicochemical properties, we used conductivity, pH, and water temperature, and excluded concentration of DO and CO₂, because they strongly relate to the main response variables of interest (i.e., stream metabolism and CO₂ exchange). Finally, for DOM quality, we used SUVA, FI, HIX, and BIX. We did not include SR, because it was strongly correlated with BIX ($r=0.89$), and we had to reduce the number of variables from this and further analyses. All variables were

scaled to unit variance and the PCA was performed using the `rda()` function in the `vegan` package (Oksanen et al. 2020).

We analyzed differences in stream metabolism using linear mixed-effect models with GPP, ER, and NEP as dependent variables, environmental variables as fixed factors, and ecoregion as the random factor to account for potential spatial autocorrelation. We first reduced the number of variables by selecting variables known to affect the response variable based on the literature (Tank et al. 2010; Hoellein et al. 2013; Bernhardt et al. 2018; Marzolf and Ardón 2021). For GPP, the selection included DIN, SRP, water temperature, discharge, and the percent of the stream reach covered by primary producers. For ER, the selection included DOC, water temperature, discharge, SUVA, HIX, BIX, GPP and the percent of the stream reach covered by primary producer. For NEP, the selection included DIN, SRP, DOC, water temperature, discharge, SUVA, HIX, BIX, and the percent of the stream reach covered by primary producers. Then, we selected the best model using backward elimination of fixed-effect terms in the linear mixed-effect models. More specifically, we used the `lmer()` and `step()` functions in the `lmerTest` R package, using Satterthwaite's method for degrees of freedom and t-statistics (Kuznetsova et al. 2017). We also analyzed the Variance Inflation Factor (VIF) for the fixed factors to avoid high multicollinearity between predictors.

We analyzed differences in $p\text{CO}_{2,w}$ and CO_2 exchange_(indirect) following the same procedure described for stream metabolism. For $p\text{CO}_{2,w}$ the fixed factors were the ones related to metabolic activity (GPP, ER), gas solubility (water temperature), alkalinity, and gas transfer (discharge and percent of the stream reach covered by macrophytes); and the random factor was again ecoregion. For CO_2 exchange_(indirect), the fixed factors were k_{600} and $p\text{CO}_2$ and the random effect was ecoregion. In this latter case, we also analyzed the variance explained by each predictor, using the `partR2()` function in the `partR2` R package (Stoffel et al. 2021).

Finally, we examined the spatial heterogeneity in CO_2 exchange within each stream using linear mixed-effect models with CO_2 exchange_(direct) as the dependent variable, habitat type as fixed factor [five levels: open water with high (i), medium (ii), or low (iii) current velocity, and emergent (iv) and submerged (v) macrophytes], and stream as random factor.

In all cases, we analyzed the distribution of the residuals visually inspecting the histograms and performing Shapiro–Wilk test, accepting normality only when $p > 0.05$. We also analyzed homogeneity of variances by plotting the model's residuals against fitted response values. These model assumptions (i.e., normal distribution of the residuals and homoscedasticity) were violated by the $p\text{CO}_{2,w}$ and CO_2 exchange_(direct) models, so these variables were log-transformed. Additionally, when models included predictor variables on very different

scales (i.e., models for ER and NEP), variables were standardized using a z-score normalization.

Results

Physicochemical characteristics

The study streams differed widely in water physicochemical characteristics, with ecoregion driving some of these differences (Table 1, Fig. 2). The first component of the PCA explained 28.8% of the variance. This PCA component was largely driven by site D18, which appeared far from the rest of the sites mainly because of its extremely high DIN concentration and maximum values of FI, BIX, and macrophyte cover. The second component of the PCA accounted for 27.8% of the variance. According to this PCA component, the tributaries of the Atlantic Ocean (D sites) were characterized by higher discharge, higher percent of agricultural land use in their basin, and higher SRP concentration with respect to the streams from the Salado basin (A sites) and tributaries of the Paraná and Río de la Plata (C sites).

Metabolism

Metabolic rates varied considerably among the study sites (Fig. 3 and Supplementary Table 2). GPP ranged from 0.4 to 6.7 $\text{g O}_2 \text{ m}^{-2} \text{ d}^{-1}$ and ER from 2.1 to 11.9 $\text{g O}_2 \text{ m}^{-2} \text{ d}^{-1}$. NEP ranged from -10.2 to 1.6 $\text{g O}_2 \text{ m}^{-2} \text{ d}^{-1}$, with 8 sites being net heterotrophic, two sites (A4 and C5) in balance, and only one site (D15) being net autotrophic.

Environmental drivers of metabolism differed among processes (Table 2). None of the explanatory fixed variables had a significant effect on GPP. However, there were differences among ecoregions, GPP being higher in the Paraná & Río de la Plata region (C sites). These differences explained 65.5% of the variance in GPP (Table 2). For ER, the best model (75.5% variance explained) included SUVA and the percent of the stream reach covered by primary producers (Table 2). Both were positively related to ER: the higher the content of aromatic carbon and the cover by primary producers, the higher the ER. Overall, ER was highest in the tributaries of the Atlantic Ocean (D sites) and lowest in the Salado River and tributaries (A sites), ecoregion accounting for 16.4% of the variance. Results for NEP were consistent, the final model (74.8% variance explained) including SUVA and the percent of the stream reach covered by primary producers (Table 2). In this case, the higher the content of aromatic carbon

Table 1 Morphological and physicochemical characteristics, macrophyte cover, and net ecosystem production (NEP) in the sampled streams; temp = temperature; NA = not available

Ecoregion	Stream code	Depth (cm)	Width (m)	Water temp (°C)	Conductivity (µS cm ⁻¹)	pH	DO (mg L ⁻¹)	Alkalinity (meq L ⁻¹)	Discharge (L s ⁻¹)	DOC (mg L ⁻¹)	SUVA (L mg ⁻¹ m ⁻¹)	SR	FI	BIX	HIX	SRP (mg L ⁻¹)	DIN (mg L ⁻¹)	Macrophyte cover (%)	NEP (mmol CO ₂ m ⁻² d ⁻¹)
Salado basin	A1	23.98	6.03	20.2	2550	8.50	7.17	8.80	120.34	6.86	19.27	0.948	2.037	0.563	6.892	0.140	0.160	0.11	-69
	A2	10.83	3.32	29.5	2129	9.87	6.84	6.27	0.86	21.60	18.13	0.933	2.083	0.599	7.513	0.011	1.927	25.31	-103
	A3	22.84	4.60	24.3	528	7.78	0.02	4.07	13.07	11.66	28.08	0.885	1.933	0.516	7.482	0.072	6.633	NA	NA
	A4	40.61	4.80	28.6	505	7.92	6.40	3.79	93.1	7.75	18.42	0.954	2.030	0.553	8.877	0.030	0.055	56.36	NA
Tributaries Paraná & Río de la Plata	C5	18.53	1.37	28.8	1205	9.00	10.55	11.08	20.57	15.47	2.62	0.868	2.031	0.603	5.587	0.119	15.457	47.84	-115
	C7	18.70	2.59	17.6	784	8.62	11.01	7.86	53.36	25.25	0.61	0.870	2.145	0.589	5.279	0.129	4.303	12.44	6
	C8	47.91	6.48	21.4	964	8.49	12.01	7.33	282.08	3.62	12.60	0.894	2.021	0.577	8.754	0.128	0.355	2.72	65
	C10	23.42	4.53	26.4	1597	8.87	13.35	10.14	54.5	2.63	10.92	1.002	2.035	0.582	6.250	0.092	1.683	27.27	-3
Tributaries Atlantic Ocean	D15	41.00	3.82	14.9	1087	8.75	11.37	8.10	150.8	9.80	42.05	0.797	1.872	0.509	8.659	0.365	1.240	4.00	-414
	D16	26.83	6.57	18	611	8.64	9.11	4.07	253.3	9.78	27.31	0.880	1.964	0.517	8.369	0.759	14.206	8.76	NA
	D17	56.75	4.58	18.3	734	8.90	8.50	4.52	279.25	8.07	27.61	0.848	1.947	0.536	7.282	0.271	0.771	6.07	-250
	D18	28.17	7.38	22.8	801	8.69	8.25	7.25	323.7	1.69	14.27	1.313	2.332	0.795	9.004	0.086	68.660	87.73	-341
	D19	51.20	5.77	16.9	1011	8.80	9.52	8.14	484.9	4.52	9.23	0.825	1.974	0.546	8.501	0.667	3.286	40.20	-50
	D20	41.78	8.97	16.1	981	8.88	9.54	7.78	434.88	8.59	2.78	0.870	1.994	0.573	7.298	0.214	4.375	12.20	-64

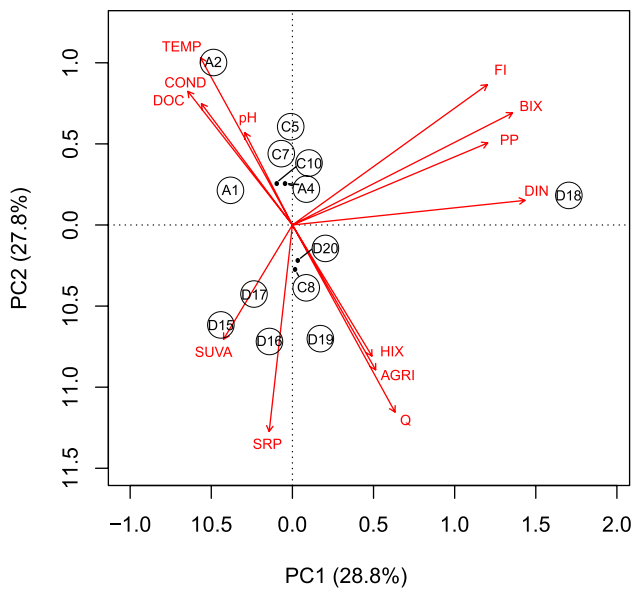


Fig. 2 Principal component analysis (PCA) of selected variables. The percent values on each axis represent the amount of variance explained by each PCA component. See Table 1 and Supplementary Table 1 for a more detailed description of the variables included in the PCA

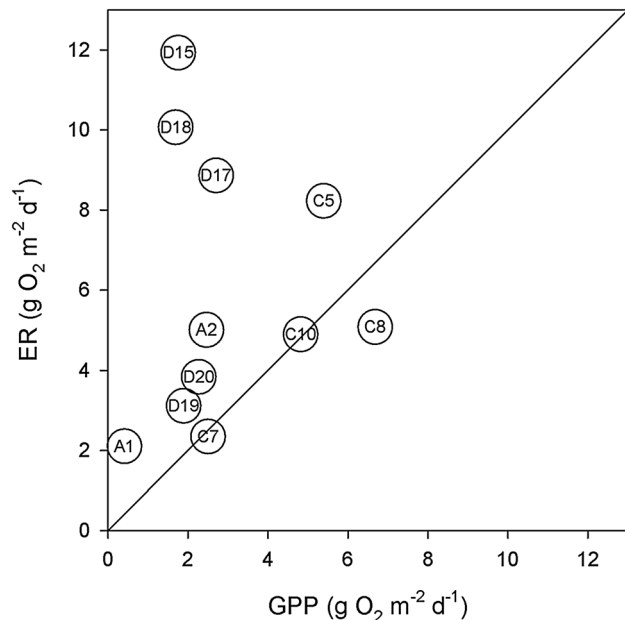


Fig. 3 Ecosystem respiration (ER) and gross primary production (GPP) in the 11 streams in which we could estimate metabolism. The solid 1:1 line describes the shift from net heterotrophy (ER > GPP) to net autotrophy (GPP > ER)

Table 2 Mixed-effects model results for metabolic rates (GPP, ER, and NEP), pCO_{2,w}, and CO₂ exchange_(indirect)

	Estimate	SE	DF	t Value	p Value
GPP					
(Intercept)	2.83	1.048	2.0	2.70	0.114
$\sigma^2/\tau_{ecoregion}$	1.49/2.83				
Marginal R^2 /conditional R^2	0.000/0.655				
ER					
(Intercept)	0.097	0.322	1.5	0.30	0.800
Macrophytes	0.526	0.193	6.3	2.72	0.033
SUVA	0.830	0.203	7.3	4.08	0.004
$\sigma^2/\tau_{ecoregion}$	0.31/0.21				
Marginal R^2 /conditional R^2	0.591/0.755				
NEP					
(Intercept)	-0.158	0.185	1.4	-0.85	0.513
Macrophytes	-0.521	0.169	7.5	-3.09	0.016
SUVA	-0.811	0.169	7.8	-4.81	0.001
$\sigma^2/\tau_{ecoregion}$	0.25/0.03				
Marginal R^2 /conditional R^2	0.721/0.748				
log(pCO_{2,w})					
(Intercept)	6.987	0.359	8.0	19.44	< 0.0001
Alkalinity	0.127	0.046	8.0	2.75	0.025
GPP	-0.112	0.044	8.0	-2.57	0.033
$\sigma^2/\tau_{ecoregion}$	0.06/0.00				
Marginal R^2 /conditional R^2	0.523/ ^a				
CO₂ exchange_(indirect)					
(Intercept)	0.521	0.198	8.0	2.63	0.030
k_{600}	0.815	0.137	8.0	5.97	< 0.001
pCO ₂	1.520	0.435	8.0	3.50	0.008
$\sigma^2/\tau_{ecoregion}$	0.19/0.00				
Marginal R^2 /conditional R^2	0.821/ ^a				
$k_{600} R^2/pCO_2 R^2$	0.637/0.219				

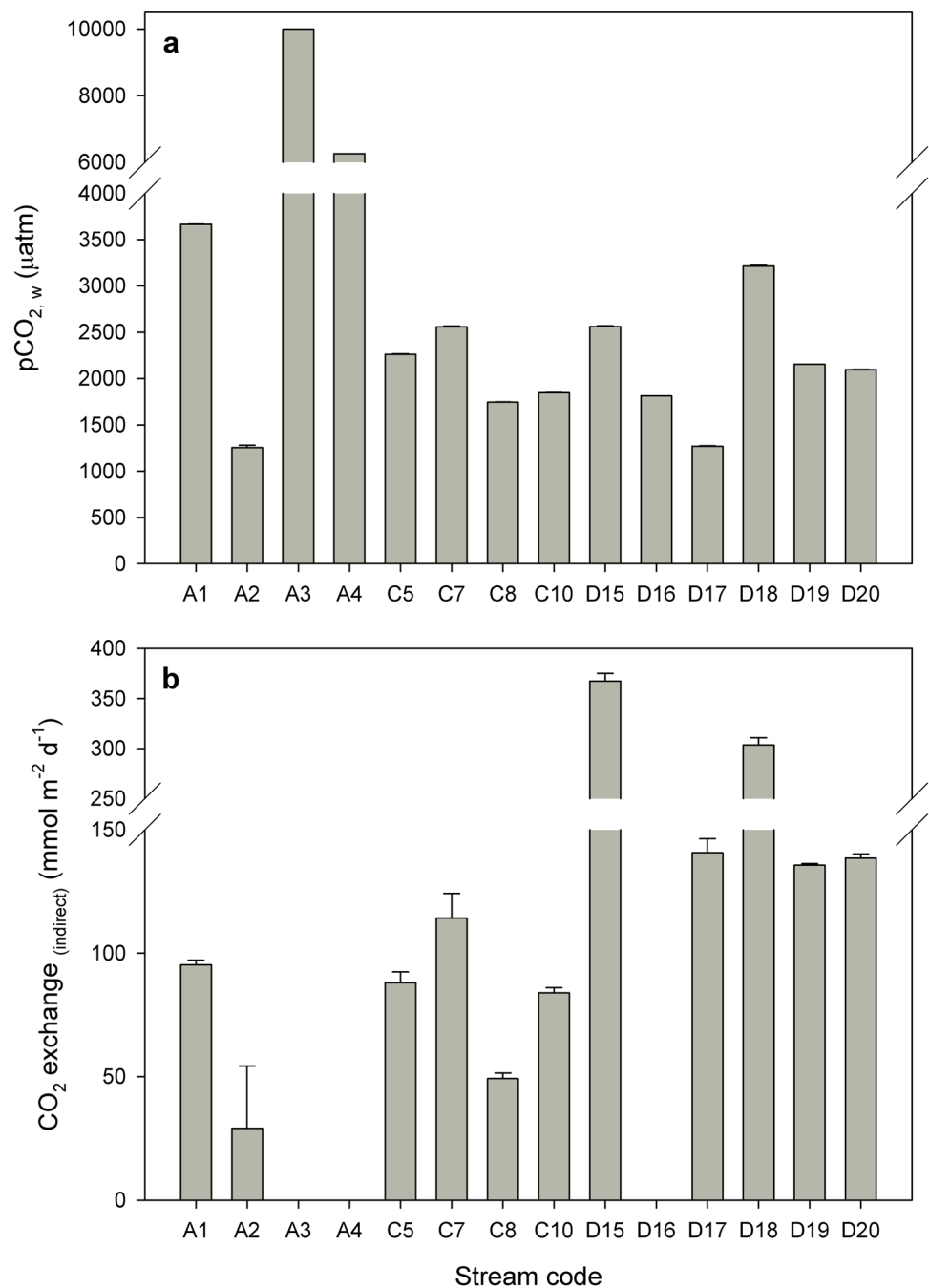
Bold value indicates the $p < 0.01$

SE standard error of each coefficient estimates, DF degrees of freedom based on the Satterthwaite's approximation, σ^2 residual variance, $\tau_{ecoregion}$ variance explained by the random factor ecoregion, Marginal R^2 proportion of variance explained by the fixed factors, Conditional R^2 proportion of variance explained by both the fixed and random factors

^aConditional R^2 is NA, because the random factor explains no variance

and the cover by primary producers, the lower the NEP (i.e., the higher the degree of heterotrophy). There were no significant differences among ecoregions (variance explained < 3%).

Fig. 4 Mean and standard deviation of **a** the partial pressure of CO₂ in water ($p\text{CO}_{2,w}$) and **b** the CO₂ exchange estimated with the indirect approach (CO₂ exchange_(indirect)) in the sampled streams. Note that some streams (A3, A4, and D16) have no CO₂ efflux due to the lack of k_{600} estimates. Also, note that some standard deviations are so small that they are hidden in the bar charts



$p\text{CO}_2$ and CO₂ exchange

All streams were CO₂ supersaturated, with $p\text{CO}_{2,w}$ values ranging from 1255 to 9999 μatm (Fig. 4a and Supplementary Table 2). Both alkalinity and GPP had a significant effect on $p\text{CO}_{2,w}$: the higher the alkalinity the higher the $p\text{CO}_{2,w}$, and the higher the GPP the lower the $p\text{CO}_{2,w}$ (Table 2). This model explained 52.3% of the variance, ecoregion accounting for none of it.

Supersaturation was reflected in positive CO₂ exchange (i.e., all streams were net emitters of CO₂ to the atmosphere), with CO₂ exchange_(indirect) values ranging from 29.1 to 367.6 $\text{mmol m}^{-2} \text{d}^{-1}$ (Fig. 4b and Supplementary Table 2). As expected, both predictor variables introduced in the model (k_{600} and $p\text{CO}_{2,w}$) had a significant positive effect on CO₂ exchange (Table 2, Fig. 5). However, k_{600} explained a higher proportion of the variance than $p\text{CO}_{2,w}$ (63.7% and 21.9%, respectively).

The spatial variability in CO₂ exchange within stream reaches was substantial (Fig. 6). CO₂ exchange_(direct) tended

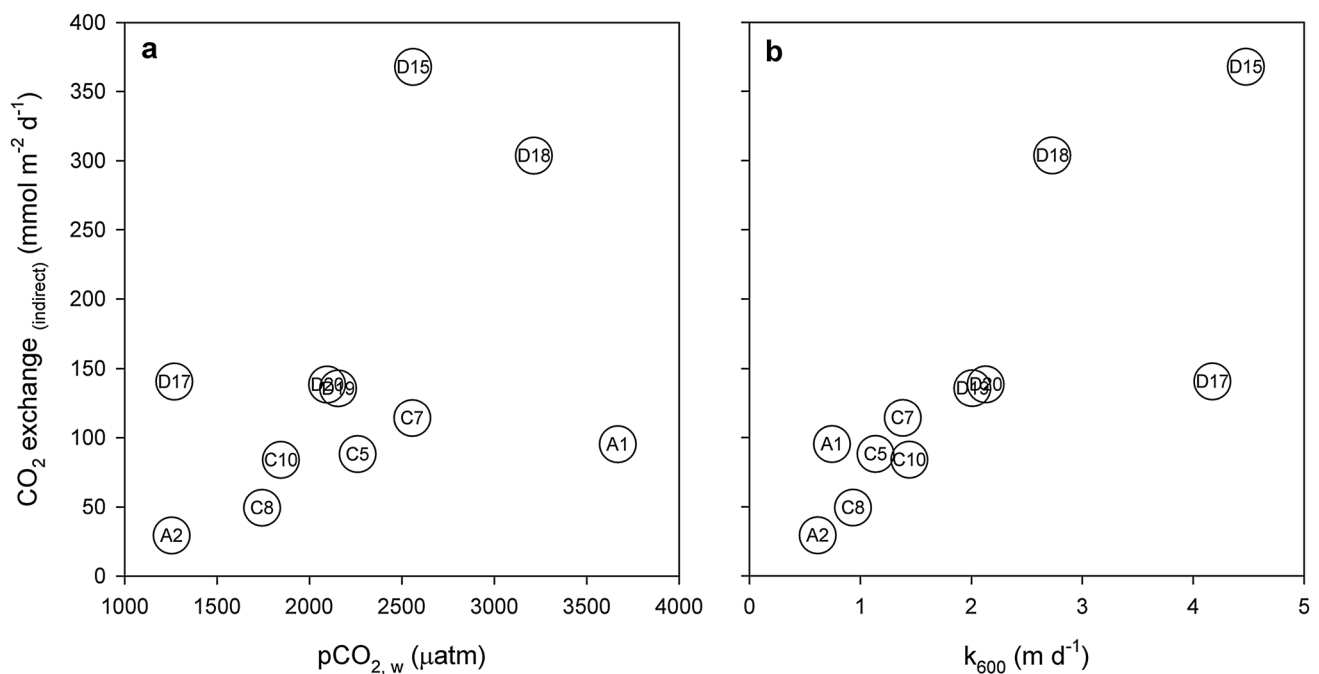


Fig. 5 Relationship between **a** CO₂ exchange estimated with the indirect approach (CO₂ exchange_(indirect)) and the partial pressure of CO₂ in water (pCO_{2,w}), and **b** CO₂ exchange_(indirect) and gas transfer velocity (k₆₀₀) in the 11 streams in which we could estimate metabolism and k₆₀₀

to be higher in sub-reaches with high current velocity and lower in sub-reaches with presence of emerged macrophytes, variability being higher within other sub-habitat types (i.e., medium and low current velocity, and submerged macrophytes; Table 3, Fig. 6).

Discussion

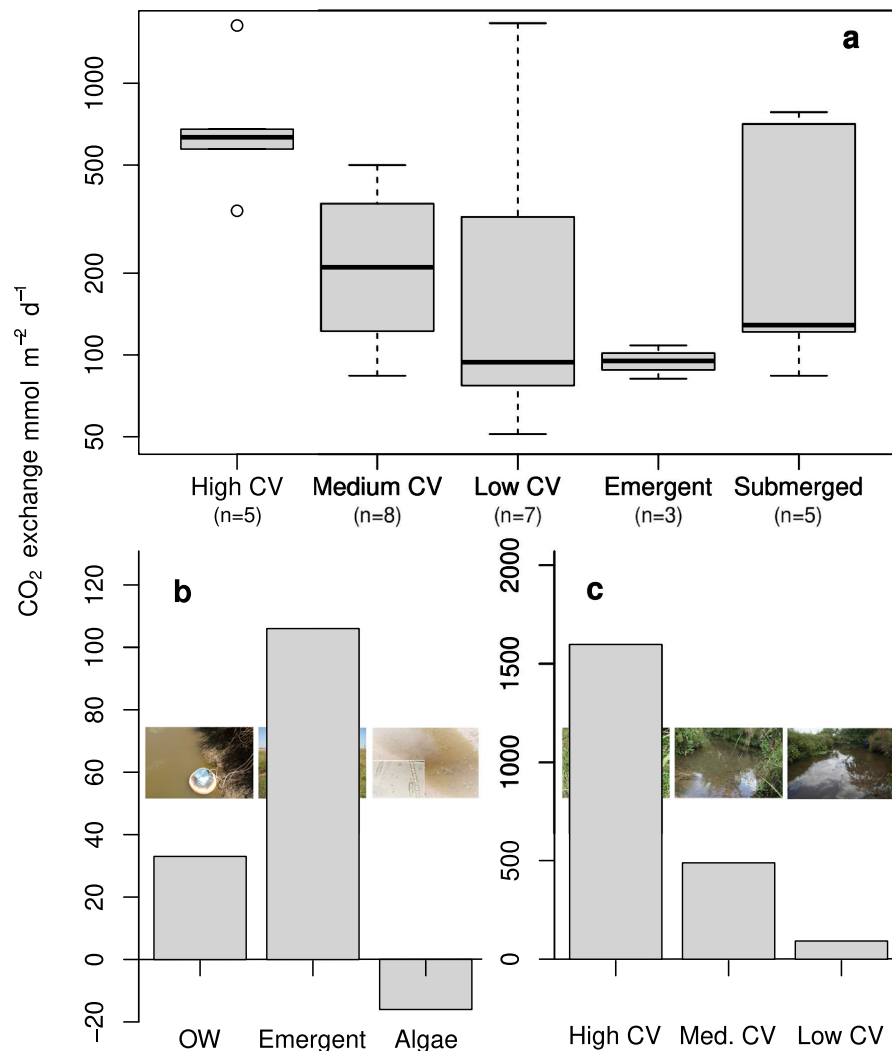
Our results confirmed that all study streams were CO₂ supersaturated and net emitters of CO₂. Internal metabolism contributed to CO₂ dynamics, although external DIC inputs via groundwater were likely important drivers of pCO_{2,w}. Despite generally high pCO_{2,w}, the slow current velocities and low water turbulence characteristic of these streams restricted CO₂ exchange with the atmosphere. Moreover, variability in both current velocity and coverage of primary producers enhanced the spatial heterogeneity of CO₂ exchange within streams.

The fact that the study streams were CO₂ supersaturated relative to the atmosphere and thus net emitters of CO₂ was expected, as most streams and rivers behave in this manner, resulting in a substantial contribution to the global carbon cycle (Raymond et al. 2013; Lauerwald et al. 2015). Our model showed that pCO_{2,w} increased with alkalinity and decreased with GPP, providing evidence that both external and internal sources of DIC drive pCO_{2,w} variation in the study streams. On the one hand, the positive relationship

between pCO_{2,w} and alkalinity suggests that mineral weathering in the catchment is an important source of DIC, which enters streams via groundwater (Feijóo et al. 2018), and probably contributes to CO₂ supersaturation in stream water (Marcé et al. 2015; Stets et al. 2017). In fact, alkalinity in the study streams varied between 3.79 and 11.08 meq L⁻¹. On the other hand, the negative relationship between pCO_{2,w} and GPP suggests that CO₂ uptake via photosynthesis by primary producers (e.g., macrophytes and algae) can reduce to some extent the concentration of CO₂ in stream water (Wallin et al. 2020). We might have expected CO₂ undersaturation in streams that were net autotrophic (GPP > ER). However, all study streams except three were net heterotrophic, and even the only net autotrophic stream (D15) was CO₂ supersaturated (pCO_{2,w} = 2561 μatm) compared to the atmosphere. These observations suggest that relative to external sources (i.e., groundwater DIC inputs originated from soil respiration and mineral weathering in the catchment), internal metabolism might be a minor driver of CO₂ concentration and exchange in these streams. This supposition is in line with previous studies, showing that internal metabolism typically accounts for a minor proportion of CO₂ outgassing from streams to the atmosphere (Butman and Raymond 2011; Hotchkiss et al. 2015; Gómez-Gener et al. 2016; Hill et al. 2017; Demars 2019).

Results from metabolism models showed that there was a positive relationship between ER (and NEP) and the cover by primary producers. Thus, and contrary to our

Fig. 6 Fine-scale spatial heterogeneity of CO₂ exchange estimated with the direct approach (CO₂ exchange_(direct)) in **a** all streams, **b** within A2, and **c** within C7. CV current velocity, OW open water



expectations, streams with a higher abundance of macrophytes showed a higher degree of heterotrophy. This could be explained by the presence of dense bacterial communities in benthic and epiphytic biofilms. Punctual estimations made in one of the study streams indicated that bacterial density in the epipelton and in the epiphyton–macrophyte complex can be high ($2.17\text{E}+08$ and $1.37\text{E}+07$ cell L⁻¹, respectively) (Ana Torremorell, pers. comm.). In addition, macrophytes tend to accumulate fine organic matter, which together with the decomposition of macrophyte tissues may enhance benthic respiration (O'Brien et al. 2014). Moreover, shading by macrophytes may limit algal productivity on sediments (Sand-Jensen et al. 1989). Together, these different macrophyte-linked processes could explain the heterotrophic character of the study streams despite the high irradiance and the abundance of primary producers.

ER was also positively related to the SUVA index, an indicator of the aromatic carbon content (Helms et al. 2008).

Several studies have shown that aromatic compounds of high molecular weight can contribute to the pool of reactive DOC, representing a relevant component of the carbon cycle in streams (Kaplan and Cory 2016). Complex molecules with aromatic groups can be photodegraded to simple compounds, increasing the bioavailability of residual DOC that is not converted into CO₂ (Fasching et al. 2014; Fovet et al. 2020). In addition, Jones et al. (2016) observed that DOM composed of humic materials is more sensitive to photodegradation. In Pampean streams, the relative contribution of humic materials to DOM is high (Messetta et al. 2018), and high irradiance conditions may favor the photodegradation of humic compounds that may be bioavailable to microbial communities. This could explain the strong relationship between ER and SUVA found in our study, and suggests that the presence of aromatic dissolved organic compounds in water fueled microbial respiration in these

Table 3 Mixed-effects model results for the spatial heterogeneity of CO₂ exchange

	Estimate	SE	DF	t Value	p Value
log(CO ₂ exchange _(direct))					
High CV (intercept)	6.51	0.405	19.5	16.07	< 0.0001
Medium CV	- 1.17	0.481	17.6	- 2.43	0.026
Low CV	- 1.34	0.532	21.8	- 2.52	0.020
Emergent macrophytes	- 1.88	0.667	18.8	- 2.81	0.011
Submerged macrophytes	- 1.05	0.570	20.8	- 1.85	0.079
$\sigma^2/\tau_{ecoregion}$	0.66/0.13				
Marginal R ² /Conditional R ²	0.284/0.402				

Bold value indicates the $p < 0.01$

CV current velocity, SE standard error of each coefficient estimates, DF degrees of freedom based on the Satterthwaite's approximation, σ^2 residual variance; $\tau_{ecoregion}$ variance explained by the random factor ecoregion, Marginal R² proportion of variance explained by the fixed factors, Conditional R² proportion of variance explained by both the fixed and random factors

streams. Macrophytes may have contributed to the release of at least part of this colored DOM (Lürig et al. 2021).

Regarding CO₂ exchange across the air–water interface of streams, as expected, we observed a significant effect of both k_{600} and pCO₂. However, in our case, k_{600} explained significantly more variance than pCO₂. This result was likely due to the extremely low turbulence of these low-gradient and slow-flowing streams (Feijóo and Lombardo 2007). The k_{600} values modeled in our study streams (0.61 to 4.47 m d⁻¹) are in the lower range of k_{600} values reported in a recent review of gas exchange in streams (range = 0.100 to 4117.8 m d⁻¹, mean = 45.0 m d⁻¹, $n = 718$; Ulseth et al. 2019). Additionally, macrophytes can form dense mats, further hampering gas exchange with the atmosphere (Attermeyer et al. 2016). Under these conditions of extremely slow gas exchange, water pCO₂ can be far from equilibrium with the atmosphere. The CO₂ in the stream, which might be fueled by groundwater DIC inputs and, to a lesser extent, by internal ER, is not compensated by the output via turbulence-limited CO₂ exchange with the atmosphere. Accordingly, as stated earlier, stream water becomes supersaturated with CO₂, even in the net autotrophic streams. Thus, overall variation in CO₂ is mostly governed by differences in turbulence, which is the limiting factor. In fact, changes in turbulence did not only explain variation among study sites, but also variation within sites. In each stream, current velocity and the presence of macrophytes controlled the spatial heterogeneity in CO₂ exchange. Consequently, we observed highest CO₂ exchange values in open water areas with the highest flow velocity, and lowest CO₂ exchange values in areas with emergent macrophytes.

Several studies have reported that macrophyte mats, and especially floating species, act as important sinks of CO₂ (O'Brien et al. 2014; Attermeyer et al. 2016; Peixoto et al. 2016). However, although generally lower than in other parts of the streams, we always observed net emission of CO₂ above macrophyte mats. In our study, macrophytes were predominantly submerged (*Myriophyllum* sp., *Elodea nuttalli*, and *Stuckenia striata*) and emergent (*Ludwigia peploides*, and *Hydrocotyle ranunculoides*) species, and only in one spot of one stream (D18), we measured CO₂ flux on a floating species (*Lemna minima*). As stated earlier, macrophytes may have strongly contributed to in-stream pCO₂ in the studied streams through their attached heterotrophic epiphytic biofilms, their shading effect on benthic algae, and the enhancement of benthic respiration via decomposing organic matter (Sand-Jensen et al. 1989; O'Brien et al. 2014; Levi et al. 2017). It is worth mentioning here that the contribution of macrophytes to CO₂ emissions may be even larger after their senescence, when large quantities of their organic tissues are decomposed within these streams.

The relative abundance of the different primary producers could also determine CO₂ fluxes. Although it was not included in the analysis, because it was a single case, we observed that in one spot of the A2 stream, where algae and cyanobacteria were dominating, CO₂ was negative, suggesting that uptake was higher than release because of photosynthesis. Consequently, the dynamics of CO₂ exchange in the air–water interface would also be influenced by the type (algae vs. macrophytes) and specific composition (in the case of macrophytes) of the dominant autotrophic community in the stream reach.

In conclusion, our findings provide interesting insights on the role of Pampean streams in CO₂ fluxes, which could be representative of other lowland streams elsewhere in the world. Overall, our results indicate that CO₂ emission in these extremely low turbulence streams is controlled by a combination of external and internal biogeochemical processes and limited atmospheric exchange (Aho et al. 2021). External groundwater inputs of DIC might be more important than internal metabolic processes in determining CO₂ concentration and fluxes at the air–water interface in these lowland streams. However, more detailed studies considering mass–balance approaches and groundwater contributions are needed to elucidate the relative importance of these and other processes (e.g., anaerobic metabolism and calcite precipitation) for controlling CO₂ dynamics in these ecosystems. Second, open-canopy streams with dense macrophyte cover may not necessarily act as net sinks of CO₂. Primary production by macrophytes may not be able to counteract the effect of external DIC inputs. In addition, the degree of heterotrophy and the presence of abundant microbial communities may also determine whether they are net sinks or emitters of CO₂ to the atmosphere. Finally, CO₂ exchange

does not only vary significantly among different streams but also within the same stream reach. In this study, CO₂ exchange was greatly influenced by reach heterogeneity, which is generated by flow variability and by the different algal, bacterial, and macrophyte communities. This highlights the need of measuring CO₂ fluxes in multiple sites within the same reach to represent the hydrological and biological heterogeneity. Similarly, it is fundamental that future studies cover broader time scales. There is a strong seasonal and diel variability in the metabolic activity of biological communities in Pampean streams (García et al. 2017; Martí et al. 2020), which, together with temporal changes in external sources, is expected to also generate high temporal variability in CO₂ concentrations. In this study, we measured CO₂ fluxes between 12 and 16 h on 1 day of the most productive season in each stream, when CO₂ concentration could be expected to be lowest in these streams. Therefore, it is crucial that future studies more accurately account for both spatial and temporal variability to better understand the role of these ecosystems in the carbon cycle.

Supplementary Information The online version contains supplementary material available at <https://doi.org/10.1007/s00027-022-00852-9>.

Acknowledgements We thank GERSOLAR and María José De Negri for providing radiation and PAR data, and INTA Balcarce and INTA Miramar for meteorological data. We also thank the Universidad Nacional de Luján for providing vehicle and driver (special thanks to Mario Pighin and Nacho Casas). Special thanks to Adonis Giorgi for helping with the sampling campaign and the methodology. Comments from the Associate Editor and the reviewers greatly helped to improve the manuscript.

Author contributions Conceptualization: DvS and CF. Methodology: DvS and MA. Formal analysis and investigation: CF, MA, DvS, LM, JA, and LR. Writing—original draft preparation: CF, MA, and DvS; writing—review and editing: MLM, JA, and LR. Funding acquisition: CF; resources: DvS and CF. Supervision: DvS.

Funding DvS. is a Serra Hünter Fellow and was additionally supported by the Catalan Government through the FORESTREAM (Forest and Stream Ecological Links: Watershed Management and Restoration) grant (2017 SGR 976). The study was funded by CONICET through two grants (Subsidio de financiamiento para Reuniones Científicas y Tecnológicas 2018 and P-UE0017).

Availability of data and materials All data generated or analyzed during this study are included in this published article and its supplementary information files. Any additional data are available from the corresponding author on request.

Code availability The R code generated during the current study is available from the corresponding author on request.

Declarations

Conflicts of interest/competing interests The authors have no conflicts of interest to declare that are relevant to the content of this article.

Ethics approval Not applicable.

Consent to participate Not applicable.

Consent for publication Not applicable.

References

- Aho KS, Hosen JD, Logozzo LA et al (2021) Highest rates of gross primary productivity maintained despite CO₂ depletion in a temperate river network. *Limnol Oceanogr Lett* 6:200–206. <https://doi.org/10.1002/lol2.10195>
- Alin SR, Rasera MDFFL, Salimon CI et al (2011) Physical controls on carbon dioxide transfer velocity and flux in low-gradient river systems and implications for regional carbon budgets. *J Geophys Res Biogeosci*. <https://doi.org/10.1029/2010JG001398>
- Allen GH, Pavelsky TM (2018) Global extent of rivers and streams. *Science* 361:585–588
- Alnoe AB, Levi PS, Baattrup-Pedersen A, Riis T (2021) Macrophytes enhance reach-scale metabolism on a daily, seasonal and annual basis in agricultural lowland streams. *Aquat Sci* 83:1–12
- APHA (2005) Standard methods for the examination of water and wastewater, 21st edn. American Public Health Association
- Appling AP, Hall RO, Arroita M, Yackulic CB (2017) streamMetabolizer: Models for estimating aquatic photosynthesis and respiration. <https://github.com/USGS-R/streamMetabolizer/tree/v0.10.1>. Accessed 15 Sept 2020
- Appling AP, Hall RO, Yackulic CB, Arroita M (2018) Overcoming equifinality: Leveraging long time series for stream metabolism estimation. *J Geophys Res G Biogeosci* 123:624–645
- Attermeyer K, Flury S, Jayakumar R et al (2016) Invasive floating macrophytes reduce greenhouse gas emissions from a small tropical lake. *Sci Rep* 6:1–10. <https://doi.org/10.1038/srep20424>
- Aufdenkampe AK, Mayorga E, Raymond PA et al (2011) Riverine coupling of biogeochemical cycles between land, oceans, and atmosphere. *Front Ecol Environ* 9:53–60. <https://doi.org/10.1890/100014>
- Bernhardt ES, Heffernan JB, Grimm NB et al (2018) The metabolic regimes of flowing waters. *Limnol Oceanogr* 63:S99–S118. <https://doi.org/10.1002/lno.10726>
- Bodmer P, Heinz M, Pusch M et al (2016) Carbon dynamics and their link to dissolved organic matter quality across contrasting stream ecosystems. *Sci Total Environ* 553:574–586. <https://doi.org/10.1016/j.scitotenv.2016.02.095>
- Butman D, Raymond PA (2011) Significant efflux of carbon dioxide from streams and rivers in the United States. *Nat Geosci* 4:839–842. <https://doi.org/10.1038/ngeo1294>
- Cole JJ, Prairie YT, Caraco NF et al (2007) Plumbing the global carbon cycle: integrating inland waters into the terrestrial carbon budget. *Ecosystems* 10:172–185
- Colt J (2012) Computation of dissolved gas concentration in water as functions of temperature, salinity and pressure, 2nd edn. Elsevier
- Cory RM, McKnight DM (2005) Fluorescence spectroscopy reveals ubiquitous presence of oxidized and reduced quinones in dissolved organic matter. *Environ Sci Technol* 39:8142–8149

- Demars BOL (2019) Hydrological pulses and burning of dissolved organic carbon by stream respiration. *Limnol Oceanogr* 64:406–421. <https://doi.org/10.1002/lno.11048>
- Duarte CM, Prairie YT (2005) Prevalence of heterotrophy and atmospheric CO₂ emissions from aquatic ecosystems. *Ecosystems* 8:862–870
- Fasching C, Behounek B, Singer GA, Battin TJ (2014) Microbial degradation of terrigenous dissolved organic matter and potential consequences for carbon cycling in brown-water streams. *Sci Rep* 4:4981
- Feijóo CS, Lombardo RJ (2007) Baseline water quality and macrophyte assemblages in Pampean streams: a regional approach. *Water Res* 41:1399–1410. <https://doi.org/10.1016/j.watres.2006.08.026>
- Feijóo C, Giorgi A, Ferreiro N (2011) Phosphate uptake in a macrophyte-rich Pampean stream. *Limnologia* 41:285–289. <https://doi.org/10.1016/j.limno.2010.11.002>
- Feijóo C, Messetta ML, Hegoburu C, Gómez-Vázquez A, Guerra-López J, Mas-Pla J, Rigacci L, García V, Butturini A (2018) Retention and release of nutrients and dissolved organic carbon in a nutrient-rich stream: a mass balance approach. *J Hydrol* 566:795–806. <https://doi.org/10.1016/j.jhydrol.2018.09.051>
- Fellman JB, Hood E, Spencer RGM (2010) Fluorescence spectroscopy opens new windows into dissolved organic matter dynamics in freshwater ecosystems: a review. *Limnol Oceanogr* 55:2452–2462. <https://doi.org/10.4319/lno.2010.55.6.2452>
- Fovet O, Cooper DM, Jones DL, Jones TG, Evans CD (2020) Dynamics of dissolved organic matter in headwaters: comparison of headwater streams with contrasting DOM and nutrient composition. *Aquat Sci* 82:29. <https://doi.org/10.1007/s00027-020-0704-6>
- Frenquelli J (1956) Rasgos generales de la hidrografía de la Provincia de Buenos Aires. *LEMIT II*:1–19
- García HR, Gordon LI (1992) Oxygen solubility in seawater: better fitting equations. *Limnol Oceanogr* 37:1307–1312
- García VJ, Gantes P, Giménez L et al (2017) High nutrient retention in chronically nutrient-rich lowland streams. *Freshw Sci* 36:26–40. <https://doi.org/10.1086/690598>
- Gardolinski PCFC, Hanrahan G, Achterberg EP et al (2001) Comparison of sample storage protocols for the determination of nutrients in natural waters. *Water Res* 35:3670–3678. [https://doi.org/10.1016/S0043-1354\(01\)00088-4](https://doi.org/10.1016/S0043-1354(01)00088-4)
- Goldenfum JA (2010) GHG measurement guidelines for freshwater reservoirs. IHA, Sutton
- Gómez-Gener L, Schiller D, Marcé R et al (2016) Low contribution of internal metabolism to carbon dioxide emissions along lotic and lentic environments of a Mediterranean fluvial network. *J Geophys Res Biogeosci* 121:3030–3044. <https://doi.org/10.1002/2016JG003549>
- Gordon ND, McMahon TA, Finlayson BL (1992) *Stream hydrology*. Wiley, Chichester
- Green SA, Blough NV (1994) Optical absorption and fluorescence properties of chromophoric dissolved organic matter in natural waters. *Limnol Oceanogr* 39:1903–1916
- Hall RO, Ulseth AJ (2020) Gas exchange in streams and rivers. *Wiley Interdiscip Rev Water* 7:e1391
- Hall RO, Tank JL, Baker MA et al (2016) Metabolism, gas exchange, and carbon spiraling in rivers. *Ecosystems* 19:73–86. <https://doi.org/10.1007/s10021-015-9918-1>
- Helms JR, Stubbins A, Ritchie JD et al (2008) Absorption spectral slopes and slope ratios as indicators of molecular weight, source, and photobleaching of chromophoric dissolved organic matter. *Limnol Oceanogr* 53:955–969
- Hill BH, Elonen CM, Herlihy AT et al (2017) A synoptic survey of microbial respiration, organic matter decomposition, and carbon efflux in US streams and rivers. *Limnol Oceanogr* 62:S147–S159
- Hoellein TJ, Bruesewitz DA, Richardson DC (2013) Revisiting Odum (1956): a synthesis of aquatic ecosystem metabolism. *Limnol Oceanogr* 58:2089–2100
- Holtgrieve GW, Schindler DE, Branch TA, A'mar ZT, (2010) Simultaneous quantification of aquatic ecosystem metabolism and reaeration using a Bayesian statistical model of oxygen dynamics. *Limnol Oceanogr* 55:1047–1063
- Hotchkiss ER, Hall RO Jr, Sponseller RA et al (2015) Sources of and processes controlling CO₂ emissions change with the size of streams and rivers. *Nat Geosci* 8:696
- Hughet A, Vacher L, Relexans S et al (2009) Properties of fluorescent dissolved organic matter in the Gironde Estuary. *Org Geochem* 40:706–719
- Johnson RK, Hering D (2009) Response of taxonomic groups in streams to gradients in resource and habitat characteristics. *J Appl Ecol* 46:175–186
- Jones JB, Mulholland PJ (1998) Carbon dioxide variation in a hardwood forest stream: an integrative measure of whole catchment soil respiration. *Ecosystems* 1:183–196. <https://doi.org/10.1007/s100219900014>
- Jones TG, Evans CD, Jones DL, Hill PW, Freeman C (2016) Transformations in DOC along a source to sea continuum; impacts of photo-degradation, biological processes and mixing. *Aquat Sci* 78:433–446. <https://doi.org/10.1007/s00027-015-0461-0>
- Kaplan LA, Cory RM (2016) Dissolved organic matter in stream ecosystems: forms, functions, and fluxes of watershed Tea. In: *Stream ecosystems in a changing environment*. Elsevier, London, pp 241–320
- Kothawala DN, Murphy K, Stedmon CA et al (2013) Inner filter correction of dissolved organic matter fluorescence. *Limnol Oceanogr Methods* 11:616–630
- Kuznetsova A, Brockhoff PB, Christensen RHB et al (2017) lmerTest package: tests in linear mixed effects models. *J Stat Softw* 82:1–26
- Lauerwald R, Laruelle GG, Hartmann J et al (2015) Spatial patterns in CO₂ evasion from the global river network. *Glob Biogeochem Cycles* 29:534–554
- Levi PS, Starnawski P, Poulsen B et al (2017) Microbial community diversity and composition varies with habitat characteristics and biofilm function in macrophyte-rich streams. *Oikos* 126:398–409
- Lu Y, Bauer JE, Canuel EA et al (2013) Photochemical and microbial alteration of dissolved organic matter in temperate headwater streams associated with different land use. *J Geophys Res Biogeosci* 118:566–580
- Lürig MD, Best RJ, Dakos V, Matthews B (2021) Submerged macrophytes affect the temporal variability of aquatic ecosystems. *Freshw Biol* 66:421–435
- Marcé R, Obrador B, Morguá J-A et al (2015) Carbonate weathering as a driver of CO₂ supersaturation in lakes. *Nat Geosci* 8:107–111
- Martí E, Feijóo C, Vilches C et al (2020) Diel variations of nutrient retention and metabolism are coupled for ammonium but not for phosphorus in a lowland stream. *Freshw Sci* 39:268–280
- Marx A, Dusek J, Jankovec J et al (2017) A review of CO₂ and associated carbon dynamics in headwater streams: a global perspective. *Rev Geophys* 55:560–585. <https://doi.org/10.1002/2016RG000547>
- Marzolf NS, Ardón M (2021) Ecosystem metabolism in tropical streams and rivers: a review and synthesis. *Limnol Oceanogr* 66:1627–1638
- Matteucci SD (2012) Ecorregión Pampa. In: Morello J et al (eds) *Ecorregiones y complejos ecosistémicos argentinos*. Editorial Orientación Gráfica Argentina, pp 391–445
- Messetta ML, Hegoburu C, Casas-Ruiz JP, Butturini A, Feijóo C (2018) Characterization and qualitative changes in DOM chemical characteristics related to hydrologic conditions in a Pampean stream. *Hydrobiologia* 808:201–217
- O'Brien JM, Lessard JL, Plew D et al (2014) Aquatic macrophytes alter metabolism and nutrient cycling in lowland streams. *Ecosystems* 17:405–417. <https://doi.org/10.1007/s10021-013-9730-8>

- Odum HT (1956) Primary production in flowing waters. *Limnol Ocean* 1:102–117
- Oksanen J, Guillaume Blanchet F, Friendly M, et al (2020) *vegan*: Community Ecology Package. R package version 2.5–7. <https://CRAN.R-project.org/package=vegan>. Accessed 15 Sept 2020
- Peixoto RB, Marotta H, Bastviken D, Enrich-Prast A (2016) Floating aquatic macrophytes can substantially offset open water CO₂ emissions from tropical floodplain lake ecosystems. *Ecosystems* 19:724–736. <https://doi.org/10.1007/s10021-016-9964-3>
- Pu J, Li J, Khadka MB et al (2017) In-stream metabolism and atmospheric carbon sequestration in a groundwater-fed karst stream. *Sci Total Environ* 579:1343–1355. <https://doi.org/10.1016/j.scitotenv.2016.11.132>
- R Core Team (2021) R: a language and environment for statistical computing. The R Foundation
- Raymond PA, Zappa CJ, Butman D et al (2012) Scaling the gas transfer velocity and hydraulic geometry in streams and small rivers. *Limnol Oceanogr Fluids Environ* 2:41–53
- Raymond P, Hartmann J, Lauerwald R et al (2013) Global carbon dioxide emissions from inland waters. *Nature* 503:355–359. <https://doi.org/10.1038/nature12760>
- Regnier P, Friedlingstein P, Ciais P et al (2013) Anthropogenic perturbation of the carbon fluxes from land to ocean. *Nat Geosci* 6:597–607. <https://doi.org/10.1038/ngeo1830>
- Sala JM, González N, Kruse E (1983) Generalización hidrológica de la Pcia. de Buenos Aires. En: *Coloquio Internacional de Hidrología de Grandes Llanuras*. Azul, pp 974–1009
- Sand-Jensen KAJ, Jeppesen E, Nielsen K et al (1989) Growth of macrophytes and ecosystem consequences in a lowland Danish stream. *Freshwat Biol* 22:15–32
- Spencer RGM, Coble PG (2014) Design for organic matter fluorescence analysis in aquatic environments. In: Coble P, Lead J, Baker A et al (eds) *Aquatic organic matter fluorescence*. Cambridge University Press, pp 125–147
- Stets EG, Butman D, McDonald CP et al (2017) Carbonate buffering and metabolic controls on carbon dioxide in rivers. *Global Biogeochem Cycles* 31:663–677
- Stoffel MA, Nakagawa S, Schielzeth H (2021) partR2: Partitioning R2 in generalized linear mixed models. *PeerJ* 9:e11414
- Tank JL, Rosi-Marshall EJ, Griffiths NA et al (2010) A review of allochthonous organic matter dynamics and metabolism in streams. *J North Am Benthol Soc* 29:118–146
- Team SD (2016) *Stan modeling language users guide and reference manual*. Team SD
- Uehlinger U, Naegeli MW (1998) Ecosystem metabolism, disturbance, and stability in a prealpine gravel bed river. *J North Am Benthol Soc* 17:165–178. <https://doi.org/10.2307/1467960>
- Ulseth AJ, Hall RO, Boix Canadell M et al (2019) Distinct air–water gas exchange regimes in low- and high-energy streams. *Nat Geosci* 12:259–263. <https://doi.org/10.1038/s41561-019-0324-8>
- Wallin MB, Audet J, Peacock M et al (2020) Carbon dioxide dynamics in an agricultural headwater stream driven by hydrology and primary production. *Biogeosciences* 17:2487–2498
- Weishaar JL, Aiken GR, Bergamaschi BA, Fram MS (2003) Evaluation of specific ultraviolet absorbance as an indicator of the chemical composition and reactivity of dissolved organic carbon. *Environ Sci Technol* 37:4702–4708

Publisher's Note Springer Nature remains neutral with regard to jurisdictional claims in published maps and institutional affiliations.